THE JOURNAL OF PHYSICAL CHEMISTRY C

Article

pubs.acs.org/JPCC

Is Molecular Rectification Caused by Asymmetric Electrode Couplings or by a Molecular Bias Drop?

Gaibo Zhang,[†,‡] Mark A. Ratner,[¶] and Matthew G. Reuter*[,‡,§,¶,∥]

[†]Oak Ridge High School, Oak Ridge, Tennessee 37830, United States

[‡]Computer Science and Mathematics Division and [§]Center for Nanophase Materials Sciences, Oak Ridge National Laboratory, Oak Ridge, Tennessee 37831, United States

[¶]Department of Chemistry, Northwestern University, Evanston, Illinois 60208, United States

Supporting Information

ABSTRACT: We investigate possible causes of molecular rectification in electrode−molecule−electrode junctions. By using a simple model and simulated conductance histograms, we show that a molecular bias drop is responsible for rectification; conversely, asymmetric molecule−electrode couplings do not directly result in rectification. Instead, the degree of coupling (a)symmetry can be observed in the line shapes of the conductance histograms used to experimentally assess the current−voltage properties of such molecular junctions. More coupling asymmetry leads to less positively skewed histogram peaks.

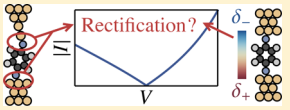

1. INTRODUCTION

Understanding how single molecules conduct electric current when connected to electrodes is interesting for both fundamental and applied reasons.[1−5] For instance, electron dynamics change when the system is driven away from equilibrium, and the ability to control electric current on molecular time and length scales may lead to improved photovoltaics, thermoelectrics, and sensors. However, tools from conventional electronics are not readily applicable to single molecules, which have an inherently quantum mechanical nature. Unlike traditional systems, molecules have a discrete number of conduction channels through which electric current can flow.[6,7] Each channel has a conductance G between 0 and $G_0 \equiv 2e^2/h$, and in this sense, a molecule exhibits quantized conductance.

Both theoretical and experimental investigations have explored the ramifications of quantized conductance over the last 20 years. Let us consider two examples. First, the molecule−electrode interfaces are critically important,[8−25] as often evidenced through the use of various chemical linker groups. It is also possible that one molecule can bind to the electrodes in several ways, each of which results in a different conductance.[10,13,16,19,20,26−29] Second, current−voltage profiles are usually non-Ohmic; that is, the conductance (alternatively, the resistance) changes with the applied bias, V.[3,30−33] In this case, both the current, I, and the differential conductance, $G \equiv dI/dV$, help to quantify the electrical response properties of the molecular junction.[31]

This non-Ohmic behavior suggests that molecules can function as rectifiers,[2,24,31,34−38] where the electric current through the molecular junction is different for positive and negative biases. Indeed, rectification has been reported through junctions containing either a single molecule or many molecules[24,39−42] (and the rectification properties can be quite different due to cooperative effects between molecules[43,44]). Many of these studies used asymmetric molecules,[2,24,34,40,41,45] where the molecule either possesses a permanent electric dipole or uses different linking groups to bind the two electrodes; however, rectification has also been demonstrated in symmetric molecules.[2,37,39,42]

Regardless of the molecular symmetry, two mechanisms have been suggested for rectification. First, some of the applied bias drops across the molecule,[24,36,37,45] indicating that the electrode−molecule−electrode junction has a (permanent or induced) dipole. In effect, the molecular channel energies change with the bias: A positive (negative) bias might bring a channel closer to resonance, thereby increasing the current, whereas a negative (positive) bias would push the channel away from resonance and decrease the current. Second, molecular asymmetry results in a molecular channel that is coupled differently to the two electrodes. Should such asymmetric couplings lead to an asymmetric electric potential profile along the molecule, rectification will be observed.[31,36,37,45]

At first glance, it may appear that the latter mechanism is inconsistent because some symmetric molecules have displayed rectification. However, common experimental techniques for measuring molecular conductance are complicated by geometric uncontrollability and irreproducibility.[9−12,15,16,27,29,32,33,42,46−60] Even though the molecule may be symmetric, a scanning tunneling microscope-based break junction experiment (for example) cannot determine the geometrical details of the measured junction,[9,12,16,50−53,57,58] let alone reliably create a perfectly symmetric junction. In all likelihood, the two electrodes will have different shapes or surface features, thus causing the couplings to be asymmetric.

Received: September 15, 2014
Revised: February 1, 2015

DOI: 10.1021/jp5093515
J. Phys. Chem. C XXXX, XXX, XXX−XXX

As another consequence of this experimental uncertainty, the electronic properties of molecules are statistically assessed from many (typically thousands or more) measurements by compiling the data into a histogram.[9,11,12,18,24,29,33,42,46−48,51,52,54,56,58,59,61−66] A conductance histogram peak not only reports the most probable conductance, for example, through the molecular junction,[9,12,15,32,46,47,57,61,67] but the statistics of the data (the peak's line shape) provide additional insight into molecular conductance.[11,14,15,29,32,48,49,57,60,64,65,67−69] For example, the zero-bias conductance histogram peak for transport through a molecule is positively skewed;[64] that is, the histogram peak has a longer tail to higher conductances than to smaller conductances.

In this work we employ a model similar to that of ref 24 to investigate the independent effects of a molecular bias drop and of asymmetric electrode couplings on electron transport properties. We find that asymmetric electrode couplings are *not* responsible, on their own, for rectification, whereas a molecular bias drop always results in rectification. We then develop and use a computational framework for simulating conductance histograms to show that the statistics in the histogram peak provide a signature for asymmetric molecule−electrode couplings. Although our results show that only a molecular bias drop is directly responsible for rectification, asymmetric electrode coupling is still encoded in experimental data.

The layout of this paper is as follows. We begin by introducing Landauer-Büttiker theory for electron transport and by developing our theory of conductance histograms in section 2. Section 3 then presents the main results, showing that a molecular bias drop causes rectification and that asymmetric electrode couplings are evident in the skewness of a conductance histogram peak. Finally, we summarize and conclude in section 4.

2. ELECTRON TRANSPORT AND CONDUCTANCE HISTOGRAMS

In this section we discuss pertinent aspects of electron transport theory (section 2.1), introduce our model system for investigating the mechanism of molecular rectification, and finally describe our framework for simulating conductance histograms (section 2.2).

2.1. Landauer-Büttiker Theory. Single electron transport theories typically employ scattering theory to describe electron dynamics.[3] When we limit our attention to elastic, coherent scattering under steady-state conditions, we obtain the Landauer-Büttiker formalism,[6,70] which is often used to describe electric current through molecules. Conduction channels are central to this formalism, and each channel has a probability of transmitting an electron with energy E from one electrode to the other. The sum of such transmission probabilities over all channels yields the transmission function, $T(E)$, to which each channel usually contributes a Lorentzian-shaped component.

All of the transport quantities we seek to understand build upon the transmission function. Consider the electric current,[3]

$$I(V) = \frac{2e}{h}\int_{-\infty}^{\infty} \mathrm{d}E\ T(E;\ V)[f_{\mathrm{L}}(E;\ V) - f_{\mathrm{R}}(E;\ V)]$$

where f_{L} (f_{R}) is the Fermi function of the left (right) electrode. Note that the Fermi functions and the transmission function generally depend on the applied bias. Because tunneling behavior is reasonably insensitive to temperature, it is convenient to work in the limit of zero temperature, where the Fermi functions become step functions. Then,

$$I(V) = \frac{2e}{h}\int_{E_{\mathrm{F}}-eV/2}^{E_{\mathrm{F}}+eV/2} \mathrm{d}E\ T(E;\ V) \tag{1}$$

where E_{F} is the Fermi energy of the electrode−molecule−electrode junction. Finally, we obtain an expression for the differential conductance by combining its definition with eq 1,

$$\begin{aligned} G(V) &\equiv \frac{\mathrm{d}}{\mathrm{d}V} I(V) \\ &= \frac{2e^2}{h}\frac{1}{2}[T(E_{\mathrm{F}} + \mathrm{eV}/2;\ V) + T(E_{\mathrm{F}} - eV/2;\ V)] \\ &\quad + \frac{2e}{h}\int_{E_{\mathrm{F}}-eV/2}^{E_{\mathrm{F}}+eV/2} \mathrm{d}E\ \frac{\partial}{\partial V} T(E;\ V) \end{aligned} \tag{2}$$

Equations 1 and 2 show how to calculate electron transport properties through an electrode−molecule−electrode junction, up to obtaining the transmission function. There are three key components that lead to $T(E)$: (i) the Hamiltonian of the isolated molecule (channel), $\mathbf{H}$; (ii) a self-energy, $\mathbf{\Sigma}_{\mathrm{L}}(E)$, describing how the isolated molecule couples to the left electrode; and (iii) a similar self-energy, $\mathbf{\Sigma}_{\mathrm{R}}(E)$, for the right electrode. Note that the self-energies are non-Hermitian operators that essentially encapsulate open-system boundary conditions. From these,[3]

$$T(E) = \mathrm{Tr}[\mathbf{G}(E)\mathbf{\Gamma}_{\mathrm{L}}(E)\mathbf{G}^{\dagger}(E)\mathbf{\Gamma}_{\mathrm{R}}(E)] \tag{3a}$$

where

$$\mathbf{G}(E) = [E\mathbf{I} - \mathbf{H} - \mathbf{\Sigma}_{\mathrm{L}}(E) - \mathbf{\Sigma}_{\mathrm{R}}(E)]^{-1} \tag{3b}$$

is the molecular Green function[71] (as modified by the electrodes), $\mathbf{I}$ is the identity operator, and

$$\mathbf{\Gamma}_{\mathrm{L/R}}(E) = i[\mathbf{\Sigma}_{\mathrm{L/R}}(E) - \mathbf{\Sigma}_{\mathrm{L/R}}^{\dagger}(E)] \tag{3c}$$

is the spectral density for coupling to the left/right electrode. We write all of these operators as matrices in the following discussion, where, for simplicity, we assume an orthonormal basis set.

Our model junction consists of a single channel that couples asymmetrically to the electrodes and drops bias. The bias drop is reflected in the bias-dependent level energy. Mathematically, $\mathbf{H} = [\varepsilon + aeV]$, $\mathbf{\Sigma}_{\mathrm{L}}(E) = [-i\Gamma_{\mathrm{L}}/2\ ]$, and $\mathbf{\Sigma}_{\mathrm{R}}(E) = [-i\Gamma_{\mathrm{R}}/2\ ]$, where ε is the channel's energy level, a is the strength of the bias drop across the channel, and $\Gamma_{\mathrm{L}} > 0$ is the channel-left electrode coupling element, and likewise for $\Gamma_{\mathrm{R}} > 0$. Using eq 3,

$$T(E) = \frac{4\Gamma_{\mathrm{L}}\Gamma_{\mathrm{R}}}{4(E - \varepsilon - aeV)^2 + (\Gamma_{\mathrm{L}} + \Gamma_{\mathrm{R}})^2} \tag{4a}$$

is Lorentzian, as expected. Then, from eqs 1 and 2,

$$\begin{aligned} I(V) = \frac{4e\Gamma_{\mathrm{L}}\Gamma_{\mathrm{R}}}{h(\Gamma_{\mathrm{L}} + \Gamma_{\mathrm{R}})}\Bigg[&\arctan\left(\frac{2[E_{\mathrm{F}} - \varepsilon + (1/2 - a)eV]}{\Gamma_{\mathrm{L}} + \Gamma_{\mathrm{R}}}\right) \\ &- \arctan\left(\frac{2[E_{\mathrm{F}} - \varepsilon - (1/2 + a)eV]}{\Gamma_{\mathrm{L}} + \Gamma_{\mathrm{R}}}\right)\Bigg] \end{aligned} \tag{4b}$$

is the current and

DOI: 10.1021/jp5093515
J. Phys. Chem. C XXXX, XXX, XXX−XXX

$$G(V) = \frac{2e^2}{h}\left[\frac{4(1/2 - a)\Gamma_L\Gamma_R}{4[E_F - \varepsilon + (1/2 - a)eV]^2 + (\Gamma_L + \Gamma_R)^2} + \frac{4(1/2 + a)\Gamma_L\Gamma_R}{4[E_F - \varepsilon - (1/2 + a)eV]^2 + (\Gamma_L + \Gamma_R)^2}\right] \quad (4c)$$

is the differential conductance. Note that this model is closely related to that of ref 24; we consider the single-channel equivalent of that two-channel model. Finally, we use the ratio

$$\xi \equiv \frac{\max(\Gamma_L, \Gamma_R)}{\min(\Gamma_L, \Gamma_R)}$$

to quantify the degree of asymmetric coupling.

2.2. Conductance Histograms as Probability Density Functions. Our theory for conductance histograms begins with the idea that the various model parameters (e.g., ε, a, Γ_L, and Γ_R) behind electron transport are random variables.[64,65,67] Figure 1 depicts this concept for a generic model junction. In

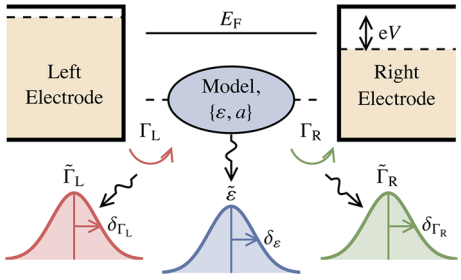

Figure 1. Schematic of our framework for simulating conductance histograms. A model system is placed between two electrodes and a bias (V) is applied across the junction. Our model system (blue) depends on the channel energy (ε) and the bias drop (a). The conduction channel in the model system couples to the left (right) electrode with Γ_L (Γ_R), and the Fermi energies of the two electrodes (dashed lines) are offset from the junction Fermi energy (E_F) by the bias. When constructing histograms, we assume that each of these physical parameters is an independent random variable. As depicted by the normal distributions, each conductance "measurement' samples from the probability distributions of these parameters.

essence, we equate the experimental irreproducibility when measuring conductance with stochasticity; each parameter has an underlying probability distribution and every measurement samples from these distributions. The conductance histogram therefore reports the probability density function[72] for the conductance observable, which is directly determined by the distributions of the model parameters.[65]

This realization facilitates the simulation of conductance histograms. Simply put, we emulate each conductance measurement by using a random number generator to sample from the model parameters' distributions (and then compute conductance as described in section 2.1). Unless otherwise specified, we use normal distributions for each parameter. Mimicking experiment, we then compile many simulated conductance values into a histogram. By changing the distributions of the parameters, we can investigate the mechanism of molecular rectification. We implemented this simulation framework for many model systems in C++11, and our software, MolStat, is available open source.[73] Specific MolStat input files for reproducing the histograms in section 3 are presented in the Supporting Information.

3. RESULTS AND DISCUSSION

Equipped with a model system that includes both asymmetric electrode couplings and a molecular bias drop, we proceed to investigate which effect leads to molecular rectification and how these effects manifest themselves in experimental data. We first examine asymmetric electrode couplings and then discuss a molecular bias drop.

3.1. Asymmetric Electrode Couplings. We start by examining the simplest system, where the molecular channel couples symmetrically to both electrodes ($\xi = 1$) and does not drop bias ($a = 0$). Mirroring ref 24, the molecular channel level is at −3 eV, the Fermi energy is 0 eV, and $\Gamma_L = \Gamma_R = 0.1$ eV. The current−voltage profile for this junction is displayed in Figure 2b and is symmetric about $V = 0$; there is no rectification. If we make the couplings less symmetric ($\xi = 2$) by increasing Γ_R to 0.2 eV, we again observe a symmetric current−voltage profile in Figure 2d. Finally, rectification remains absent if the couplings are made even more asymmetric, $\Gamma_R = 0.4$ eV (hence $\xi = 4$), in Figure 2e.

It seems doubtful from these simulations that asymmetry in the molecule−electrode couplings is, on its own, responsible for rectification. Before exploring the effects of a molecular bias drop, however, we show that coupling asymmetry is instead encoded in the statistics of experimental measurements.

To see this, we first consider the transmission spectra of the same three junctions, which are shown in Figure 2a. As expected, each transmission spectrum exhibits the characteristic Lorentzian line shape for transport through a single channel. When the coupling is symmetric (red line), the Lorentzian peaks at 1, indicating the channel's resonance energy, and asymptotically decays for energies away from the resonance. As the coupling becomes more asymmetric ($\xi = 2$ in green and $\xi = 4$ in blue), the peak decreases in magnitude and the tails decay less rapidly. In all, the transmission spectrum becomes flatter as the couplings become more asymmetric.

It has previously been shown[64,65] that the line shape of a conductance histogram peak reflects the shape of the transmission function near the Fermi energy. The argument is as follows. The fluctuations inherent to each experimental measurement cause us to sample different points on the transmission spectrum near E_F. For transport via nonresonant tunneling (where E_F is in the Lorentzian tails), $T(E)$ rises with E more quickly than it falls in this neighborhood. Consequently, fluctuations are slightly more likely to increase the transmission, resulting in a positively skewed histogram peak.[64] Transmission spectra with flatter tails will be more insulated from this effect; larger fluctuations will be required to noticeably change the observed transmission. We should, therefore, expect that junctions with increasingly asymmetric couplings will yield less skewed conductance histogram peaks.

Our conductance histogram simulation procedure (section 2.2) will now be used to demonstrate this effect. We assume ε, Γ_L, and Γ_R are random variables with normal distributions and proceed to simulate 1 million conductance "measurements" for each system. The average values of each parameter are taken to be the values used in the respective transmission spectra and current−voltage profiles. Full details on simulating these histograms can be found in the Supporting Information.

To start, Figure 2b shows a histogram where $\Gamma_L = \Gamma_R$ in every "measurement," ensuring symmetric coupling. The histogram has a bowl shape that is symmetric about $V = 0$ V, which is consistent with ref 42. In contrast, Figure 2c shows a histogram

DOI: 10.1021/jp5093515
J. Phys. Chem. C XXXX, XXX, XXX−XXX

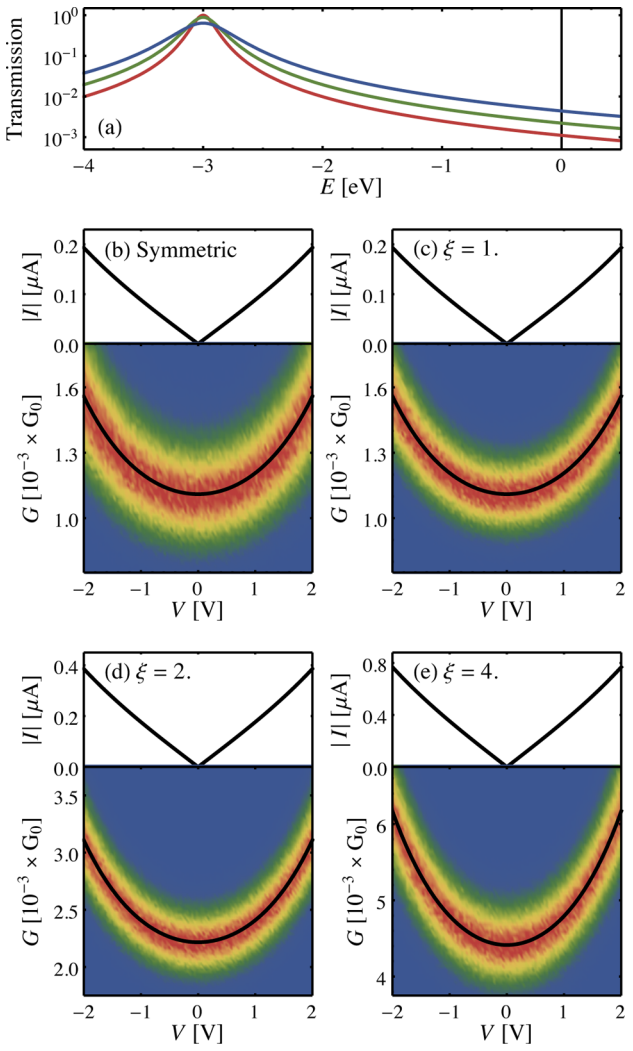

Figure 2. Electron transport properties for molecules that do not drop bias ($a = 0$). (a) Transmission spectra of channels with $\varepsilon = -3$ eV and varying degrees of coupling asymmetry. Red, $\xi = 1$; green, $\xi = 2$; blue, $\xi = 4$. The vertical line shows the Fermi energy ($E_F = 0$ eV) used for calculating current and conductance. (b)−(e) Simulated current−voltage profile (top) and conductance profile (black line, bottom) for the above channels. The bottom panel also displays a simulated conductance histogram for each channel. Red (blue) indicates a large (small) probability of observing the conductance; the absolute scale is arbitrary. In (b), $\Gamma_L = \Gamma_R$ in every sample; in (c)−(e), Γ_L and Γ_R are independently drawn from their distributions. In all cases, the current−voltage profile is symmetric about $V = 0$ V; asymmetric coupling does not result in rectification.

with the same average parameters, but where Γ_L and Γ_R are independently chosen from the same distribution. The couplings are the same, on average, but are likely to be slightly different from each other in any particular "measurement." Most noticeably, the width of the histogram peak (at a given bias) is considerably smaller than that in Figure 2b. When $\Gamma_L = \Gamma_R$ for every "measurement," smaller (larger) conductances become more probable because the electrode couplings are simultaneously small (large). The likelihood of having simultaneously small (large) couplings decreases when the two couplings are independent, resulting in a narrower histogram peak.

We now increase the degree of asymmetry in the couplings to $\xi = 2$ and $\xi = 4$ and show the resulting histograms in Figure 2d,e. When $\xi = 2$, asymmetric couplings are more prevalent in any particular "measurement," but there is still a reasonable chance that $\Gamma_L \approx \Gamma_R$ for some samples. It is unlikely that $\Gamma_L \approx \Gamma_R$ when $\xi = 4$. Unsurprisingly, both histograms are qualitatively similar to those already discussed.

Finally, Figure 3a shows the skewness of the histogram peaks in Figure 2 as a function of the bias; that is, each skewness

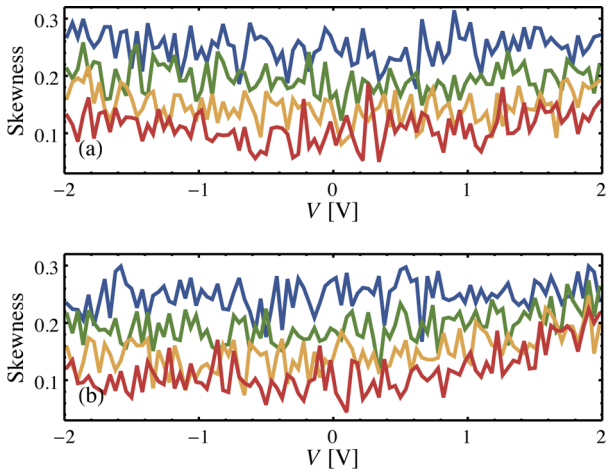

Figure 3. Skewness of the histogram peak as a function of the bias for the conductance histograms in (a) Figure 2 and (b) Figure 4. In both panels: blue is a junction where $\Gamma_L = \Gamma_R$ for every sample [panel (b) in Figures 2 and 4], green is $\xi = 1$, where Γ_L and Γ_R are the same, on average [panel (c) in Figures 2 and 4]; yellow is $\xi = 2$ [panel (d) in Figures 2 and 4]; and red is $\xi = 4$ [panel (e) in Figures 2 and 4]. As coupling asymmetry increases ($\xi \to \infty$), the skewness of the histogram peak decreases (on average).

reports the statistics from a vertical slice of a voltage-dependent conductance histogram. As expected,[64] the histogram peaks are positively skewed. Although there is some fluctuation in the skewness from one bias to another, it is apparent that the skewness decreases, on average, as ξ increases. Coupling asymmetry, while not responsible for rectification in the current−voltage profiles, can be seen in the skewness of conductance histogram peaks.

3.2. Molecular Bias Drop. We now turn to the impact of a molecular bias drop ($a \neq 0$) on the molecule's electron transport properties. Mirroring the previous discussion on coupling asymmetry, Figure 4b shows the current−voltage profile for a molecule that symmetrically couples to the electrodes and drops bias ($a = 0.15$). Because both $a > 0$ and $E_F > \varepsilon$, positive biases move the molecular channel closer to resonance; see Figure 4a, whereas negative biases push it further away. Changing to either $a < 0$ or $E_F < \varepsilon$ would lead to the opposite behavior. Consequently, the current increases more rapidly for positive biases and rectification is observed (albeit weak in this example system).

Our data suggests, therefore, that a molecular bias drop will lead to rectification. Putting all of these results together, Figure 4d,e shows the current−voltage profiles for molecules that couple asymmetrically to the electrodes *and* drop bias. As observed in ref 24, these systems still exhibit rectification. Finally, Figure 3b confirms that the skewnesses of the associated histogram peaks also reflect the coupling asymmetry.

DOI: 10.1021/jp5093515
J. Phys. Chem. C XXXX, XXX, XXX−XXX

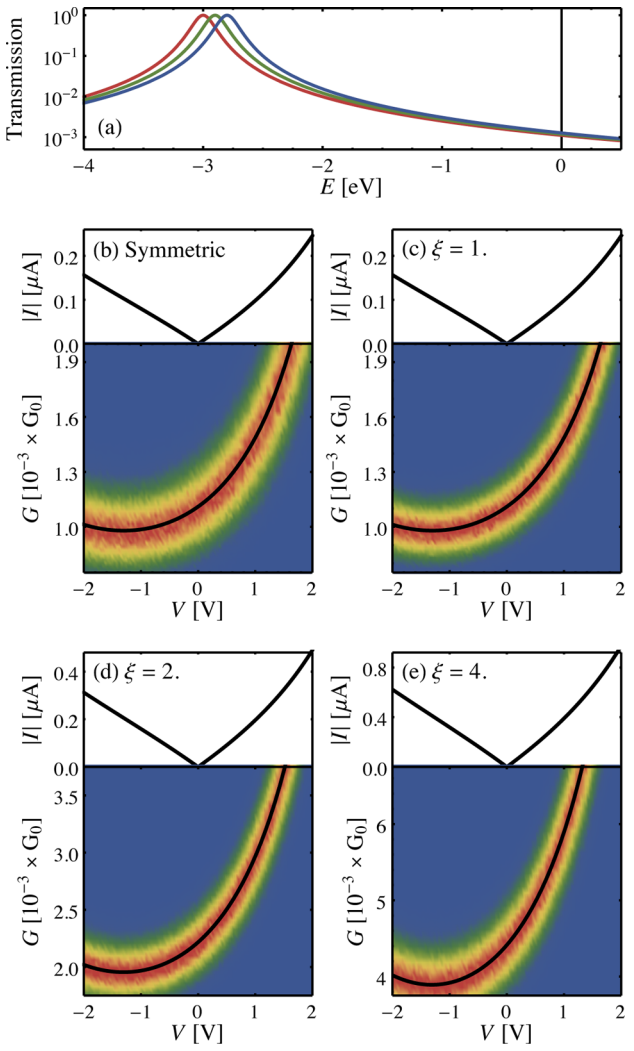

Figure 4. Electron transport properties for molecules that drop bias ($a \neq 0$). Apart from taking $a = 0.15$, all parameters are the same as in Figure 2 and the panels are similarly arranged. (a) Transmission spectrum for a channel that couples symmetrically to both electrodes and drops bias at 0 V (red), 1 V (green), and 2 V (blue). Positive (negative) biases shift the resonance to more positive (negative) energies such that the current−voltage profiles are not symmetric about $V = 0$ V. In all cases, the molecular bias drop across results in rectification.

4. CONCLUSIONS

In this work we investigated the cause of rectification in molecular junctions. Previous works have suggested two mechanisms: (i) a bias drop across the molecule and/or (ii) asymmetric couplings between the molecule and the electrodes. However, none of these studies examined the independent effects of these mechanisms, making it difficult to conclusively infer the cause of rectification. Our model, which is similar to those used before, showed that a molecular bias drop, and *not* asymmetry in the electrode couplings, is responsible for rectification. Instead, asymmetric electrode couplings lead to less positively skewed peaks in the experimental conductance histogram. This last point accentuates the high information content of conductance histogram line shapes.

We end this discussion by noting that asymmetric electrode couplings may indirectly lead to rectification, even though they are not directly responsible for it. A bias drop across the molecule can be attributed to a (permanent or induced) dipole in the molecular junction. It is probable that the different linker groups used to produce asymmetric couplings may also lead to different induced dipoles with an applied bias. The change in induced dipole from one system to the next might then change the rectification ratio of the junction, giving the illusion that asymmetric couplings lead to rectification.

■ ASSOCIATED CONTENT

Ⓢ Supporting Information

The MolStat[73] input files used to generate the histograms analyzed in Figures 2 and 4. This material is available free of charge via the Internet at http://pubs.acs.org/.

■ AUTHOR INFORMATION

Corresponding Author

*Phone: (631) 632-8198. E-mail: matthew.reuter@stonybrook.edu.

Present Address

‖Department of Applied Mathematics and Statistics and Institute for Advanced Computational Science, Stony Brook University, Stony Brook, NY 11794, United States.

Notes

The authors declare no competing financial interest.

■ ACKNOWLEDGMENTS

We thank Nongjian Tao and Latha Venkataraman for helpful conversations. G.Z. performed this research as part of a Math-Science Senior Thesis at the Oak Ridge High School. M.G.R. was supported by a Eugene P. Wigner Fellowship while at the Oak Ridge National Laboratory, which is managed by UT-Battelle, LLC, for the U.S. Department of Energy under Contract DE-AC05-00OR22725. M.A.R. and M.G.R. (while at Northwestern) were supported by the U.S. Air Force Office of Scientific Research Multidisciplinary University Research Initiative (FA9550-14-1-003). M.A.R. also thanks the Chemistry Division of the U.S. National Science Foundation for support (CHE-1058896). The figures were prepared with the SciDraw package.[74]

■ REFERENCES

(1) Nitzan, A.; Ratner, M. A. Electron Transport in Molecular Wire Junctions. *Science* **2003**, *300*, 1384−1389.
(2) Metzger, R. M. Unimolecular Electronics. *J. Mater. Chem.* **2008**, *18*, 4364−4396.
(3) Cuevas, J. C.; Scheer, E. *Molecular Electronics*; World Scientific: Hackensack, NJ, 2010.
(4) Karthäuser, S. Control of Molecule-Based Transport for Future Molecular Devices. *J. Phys.: Condens. Matter* **2011**, *23*, 013001.
(5) Ratner, M. A Brief History of Molecular Electronics. *Nat. Nanotechnol.* **2013**, *8*, 378−381.
(6) Imry, Y.; Landauer, R. Conductance Viewed as Transmission. *Rev. Mod. Phys.* **1999**, *71*, S306−S312.
(7) Paulsson, M.; Brandbyge, M. Transmission Eigenchannels from Nonequilibrium Green's Functions. *Phys. Rev. B* **2007**, *76*, 115117.
(8) Yaliraki, S. N.; Ratner, M. A. Molecule-Interface Coupling Effects on Electronic Transport in Molecular Wires. *J. Chem. Phys.* **1998**, *109*, 5036−5043.
(9) Xu, B.; Tao, N. J. Measurement of Single-Molecule Resistance by Repeated Formation of Molecular Junctions. *Science* **2003**, *301*, 1221−1223.
(10) Li, X.; He, J.; Hihath, J.; Xu, B.; Lindsay, S. M.; Tao, N. Conductance of Single Alkanedithiols: Conduction Mechanism and

DOI: 10.1021/jp5093515
J. Phys. Chem. C XXXX, XXX, XXX−XXX

Effect of Molecule−Electrode Contacts. *J. Am. Chem. Soc.* **2006**, *128*, 2135−2141.
(11) Venkataraman, L.; Klare, J. E.; Tam, I. W.; Nuckolls, C.; Hybertsen, M. S.; Steigerwald, M. L. Single-Molecule Circuits with Well-Defined Molecular Conductance. *Nano Lett.* **2006**, *6*, 458−462.
(12) Chen, F.; Hihath, J.; Huang, Z.; Li, X.; Tao, N. J. Measurement of Single-Molecule Conductance. *Annu. Rev. Phys. Chem.* **2007**, *58*, 535−564.
(13) Li, C.; Pobelov, I.; Wandlowski, T.; Bagrets, A.; Arnold, A.; Evers, F. Charge Transport in Single Au−Alkanedithiol−Au Junctions: Coordination Geometries and Conformational Degrees of Freedom. *J. Am. Chem. Soc.* **2008**, *130*, 318−326.
(14) Andrews, D. Q.; Van Duyne, R. P.; Ratner, M. A. Stochastic Modulation in Molecular Electronic Transport Junctions: Molecular Dynamics Coupled with Charge Transport Calculations. *Nano Lett.* **2008**, *8*, 1120−1126.
(15) Hybertsen, M. S.; Venkataraman, L.; Klare, J. E.; Whalley, A. C.; Steigerwald, M. L.; Nuckolls, C. Amine-Linked Single-Molecule Circuits: Systematic Trends Across Molecular Families. *J. Phys.: Condens. Matter* **2008**, *20*, 374115.
(16) Haiss, W.; Martín, S.; Leary, E.; van Zalinge, H.; Higgins, S. J.; Bouffier, L.; Nichols, R. J. Impact of Junction Formation Method and Surface Roughness on Single Molecule Conductance. *J. Phys. Chem. C* **2009**, *113*, 5823−5833.
(17) Paulsson, M.; Krag, C.; Frederiksen, T.; Brandbyge, M. Conductance of Alkanedithiol Single-Molecule Junctions: A Molecular Dynamics Study. *Nano Lett.* **2009**, *9*, 117−121.
(18) Hong, W.; Manrique, D. Z.; Moreno-García, P.; Gulcur, M.; Mishchenko, A.; Lambert, C. J.; Bryce, M. R.; Wandlowski, T. Single Molecular Conductance of Tolanes: Experimental and Theoretical Study on the Junction Evolution Dependent on the Anchoring Group. *J. Am. Chem. Soc.* **2012**, *134*, 2292−2304.
(19) Paz, S. A.; Michoff, M. E. Z.; Negre, C. F. A.; Olmos-Asar, J. A.; Mariscal, M. M.; Sánchez, C. G.; Leiva, E. P. M. Anchoring Sites to the STM Tip Can Explain Multiple Peaks in Single Molecule Conductance Histograms. *Phys. Chem. Chem. Phys.* **2013**, *15*, 1526−1531.
(20) Konishi, T.; Kiguchi, M.; Takase, M.; Nagasawa, F.; Nabika, H.; Ikeda, K.; Uosaki, K.; Ueno, K.; Misawa, H.; Murakoshi, K. Single Molecule Dynamics at a Mechanically Controllable Break Junction in Solution at Room Temperature. *J. Am. Chem. Soc.* **2013**, *135*, 1009−1014.
(21) French, W. R.; Iacovella, C. R.; Rungger, I.; Souza, A. M.; Sanvito, S.; Cummings, P. T. Structural Origins of Conductance Fluctuations in Gold-Thiolate Molecular Transport Junctions. *J. Phys. Chem. Lett.* **2013**, *4*, 887−891.
(22) Hihath, J.; Tao, N. The Role of Molecule-Electrode Contact in Single-Molecule Electronics. *Semicond. Sci. Technol.* **2014**, *29*, 054007.
(23) Ding, W.; Negre, C. F. A.; Vogt, L.; Batista, V. S. High-Conductance Conformers in Histograms of Single-Molecule Current-Voltage Characteristics. *J. Phys. Chem. C* **2014**, *118*, 8316−8321.
(24) Batra, A.; Darancet, P.; Chen, Q.; Meisner, J. S.; Widawsky, J. R.; Neaton, J. B.; Nuckolls, C.; Venkataraman, L. Tuning Rectification in Single-Molecular Diodes. *Nano Lett.* **2013**, *13*, 6233−6237.
(25) Afsari, L.; Li, Z.; Borguet, E. Orientation-Controlled Single-Molecule Junctions. *Angew. Chem., Int. Ed.* **2014**, *53*, 9771−9774.
(26) Bilić, A.; Reimers, J. R.; Hush, N. S. The Structure, Energetics, and Nature of the Chemical Bonding of Phenylthiol Adsorbed on the Au(111) Surface: Implications for Density-Functional Calculations of Molecular-Electronic Conduction. *J. Chem. Phys.* **2005**, *122*, 094708.
(27) He, J.; Sankey, O.; Lee, M.; Tao, N.; Li, X.; Lindsay, S. Measuring Single Molecule Conductance with Break Junctions. *Faraday Discuss.* **2006**, *131*, 145−154.
(28) Meisner, J. S.; Ahn, S.; Aradhya, S. V.; Krikorian, M.; Parameswaran, R.; Steigerwald, M.; Venkataraman, L.; Nuckolls, C. Importance of Direct Metal-π Coupling in Electronic Transport Through Conjugated Single-Molecule Junctions. *J. Am. Chem. Soc.* **2012**, *134*, 20440−20445.
(29) Kim, T.; Darancet, P.; Widawsky, J. R.; Kotiuga, M.; Quek, S. Y.; Neaton, J. B.; Venkataraman, L. Determination of Energy Level Alignment and Coupling Strength in 4,4′-Bipyridine Single-Molecule Junctions. *Nano Lett.* **2014**, *14*, 794−798.
(30) Mujica, V.; Kemp, M.; Roitberg, A.; Ratner, M. A. Current-Voltage Characteristics of Molecular Wires: Eigenvalue Staircase, Coulomb Blockade, and Rectification. *J. Chem. Phys.* **1996**, *104*, 7296−7305.
(31) Tian, W.; Datta, S.; Hong, S.; Reifenberger, R.; Henderson, J. I.; Kubiak, C. P. Conductance Spectra of Molecular Wires. *J. Chem. Phys.* **1998**, *109*, 2874−2882.
(32) Xiao, X.; Xu, B.; Tao, N. J. Measurement of Single Molecule Conductance: Benzenedithiol and Benzenedimethanethiol. *Nano Lett.* **2004**, *4*, 267−271.
(33) Lörtscher, E.; Weber, H. B.; Riel, H. Statistical Approach to Investigating Transport through Single Molecules. *Phys. Rev. Lett.* **2007**, *98*, 176807.
(34) Aviram, A.; Ratner, M. A. Molecular Rectifiers. *Chem. Phys. Lett.* **1974**, *29*, 277−283.
(35) Taylor, J.; Brandbyge, M.; Stokbro, K. Theory of Rectification in Tour Wires: The Role of Electrode Coupling. *Phys. Rev. Lett.* **2002**, *89*, 138301.
(36) Metzger, R. M. Unimolecular Rectifiers:Present Status. *Chem. Phys.* **2006**, *326*, 176−187.
(37) Lörtscher, E.; Gotsmann, B.; Lee, Y.; Yu, L.; Rettner, C.; Riel, H. Transport Properties of a Single-Molecule Diode. *ACS Nano* **2012**, *6*, 4931−4939.
(38) Barone, V.; Cacelli, I.; Ferretti, A.; Visciarelli, M. Theoretical Study of a Molecular Junction with Asymmetric Current/Voltage Characteristics. *Chem. Phys. Lett.* **2012**, *549*, 1−5.
(39) Dhirani, A.; Lin, P.-H.; Guyot-Sionnest, P.; Zehner, R. W.; Sita, L. R. Self-Assembled Molecular Rectifiers. *J. Chem. Phys.* **1997**, *106*, 5249−5253.
(40) Elbing, M.; Ochs, R.; Koentopp, M.; Fischer, M.; von Hänisch, C.; Weigend, F.; Evers, F.; Weber, H. B.; Mayor, M. A Single-Molecule Diode. *Proc. Nat. Acad. Sci. (USA)* **2005**, *102*, 8815−8820.
(41) Díez-Pérez, I.; Hihath, J.; Lee, Y.; Yu, L.; Adamska, L.; Kozhushner, M. A.; Oleynik, I. I.; Tao, N. Rectification and Stability of a Single Molecular Diode with Controlled Orientation. *Nat. Chem.* **2009**, *1*, 635−641.
(42) Guo, S.; Hihath, J.; Díez-Pérez, I.; Tao, N. Measurement and Statistical Analysis of Single-Molecule Current-Voltage Characteristics, Transition Voltage Spectroscopy, and Tunneling Barrier Height. *J. Am. Chem. Soc.* **2011**, *133*, 19189−19197.
(43) Nijhuis, C. A.; Reus, W. F.; Whitesides, G. M. Molecular Rectification in Metal−SAM−Metal Oxide−Metal Junctions. *J. Am. Chem. Soc.* **2009**, *131*, 17814−17827.
(44) Mirjani, F.; Thijssen, J. M.; Whitesides, G. M.; Ratner, M. A. Charge Transport Across Insulating Self-Assembled Monolayers: Non-Equilibrium Approaches and Modeling to Relate Current and Molecular Structure. *ACS Nano* **2014**, *8*, 12428−12436.
(45) Ding, W.; Negre, C. F. A.; Vogt, L.; Batista, V. S. Single Molecule Rectification Induced by the Asymmetry of a Single Frontier Orbital. *J. Chem. Theory Comput.* **2014**, *10*, 3393−3400.
(46) Haiss, W.; Nichols, R. J.; van Zalinge, H.; Higgins, S. J.; Bethell, D.; Schiffrin, D. J. Measurement of Single Molecule Conductivity using the Spontaneous Formation of Molecular Wires. *Phys. Chem. Chem. Phys.* **2004**, *6*, 4330−4337.
(47) Mayor, M.; Weber, H. B. Statistical Analysis of Single-Molecule Junctions. *Angew. Chem., Int. Ed.* **2004**, *43*, 2882−2884.
(48) Engelkes, V. B.; Beebe, J. M.; Frisbie, C. D. Analysis of the Causes of Variance in Resistance Measurements on Metal−Molecule−Metal Junctions Formed by Conducting-Probe Atomic Force Microscopy. *J. Phys. Chem. B* **2005**, *109*, 16801−16810.
(49) Ulrich, J.; Esrail, D.; Pontius, W.; Venkataraman, L.; Millar, D.; Doerrer, L. H. Variability of Conductance in Molecular Junctions. *J. Phys. Chem. B* **2006**, *110*, 2462−2466.
(50) Venkataraman, L.; Klare, J. E.; Nuckolls, C.; Hybertsen, M. S.; Steigerwald, M. L. Dependence of Single-Molecule Junction Conductance on Molecular Conformation. *Nature* **2006**, *442*, 904−907.

DOI: 10.1021/jp5093515
J. Phys. Chem. C XXXX, XXX, XXX−XXX

(51) Jang, S.-Y.; Reddy, P.; Majumdar, A.; Segalman, R. A. Interpretation of Stochastic Events in Single Molecule Conductance Measurements. *Nano Lett.* **2006**, *6*, 2362−2367.
(52) González, M. T.; Wu, S.; Huber, R.; van der Molen, S. J.; Schönenberger, C.; Calame, M. Electrical Conductance of Molecular Junctions by a Robust Statistical Analysis. *Nano Lett.* **2006**, *6*, 2238−2242.
(53) Nichols, R. J.; Haiss, W.; Higgins, S. J.; Leary, E.; Martín, S.; Bethell, D. The Experimental Determination of the Conductance of Single Molecules. *Phys. Chem. Chem. Phys.* **2010**, *12*, 2801−2815.
(54) Hong, W.; Valkenier, H.; Mészáros, G.; Manrique, D. Z.; Mishchenko, A.; Putz, A.; García, P. M.; Lambert, C. J.; Hummelen, J. C.; Wandlowski, T. An MCBJ Case Study: The Influence of π-Conjugation on the Single-Molecule Conductance at a Solid/Liquid Interface. *Beilstein J. Nanotechnol.* **2011**, *2*, 699−713.
(55) Leary, E.; González, M. T.; van der Pol, C.; Bryce, M. R.; Filippone, S.; Martín, N.; Rubio-Bollinger, G.; Agraït, N. Unambiguous *One*-Molecule Conductance Measurements under Ambient Conditions. *Nano Lett.* **2011**, *11*, 2236−2241.
(56) Guédon, C. M.; Valkenier, H.; Markussen, T.; Thygesen, K. S.; Hummelen, J. C.; van der Molen, S. J. Observation of Quantum Interference in Molecular Charge Transport. *Nat. Nanotechnol.* **2012**, *7*, 305−309.
(57) Natelson, D. Mechanical Break Junctions: Enormous Information in a Nanoscale Package. *ACS Nano* **2012**, *6*, 2871−2876.
(58) Makk, P.; Tomaszewski, D.; Martinek, J.; Balogh, Z.; Csonka, S.; Wawrzyniak, M.; Frei, M.; Venkataraman, L.; Halbritter, A. Correlation Analysis of Atomic and Single-Molecule Junction Conductance. *ACS Nano* **2012**, *6*, 3411−3423.
(59) Arroyo, C. R.; Tarkuc, S.; Frisenda, R.; Seldenthuis, J. S.; Woerde, C. H. M.; Eelkema, R.; Grozema, F. C.; van der Zant, H. S. J. Signatures of Quantum Interference Effects on Charge Transport Through a Single Benzene Ring. *Angew. Chem., Int. Ed.* **2013**, *52*, 3152−3155.
(60) Frisenda, R.; Perrin, M. L.; Valkenier, H.; Hummelen, J. C.; van der Zant, H. S. J. Statistical Analysis of Single-Molecule Breaking Traces. *Phys. Status Solidi (B)* **2013**, *250*, 2431−2436.
(61) Krans, J. M.; van Ruitenbeek, J. M.; Fisun, V. V.; Yanson, I. K.; de Jongh, L. J. The Signature of Conductance Quantization in Metallic Point Contacts. *Nature* **1995**, *375*, 767−769.
(62) Halbritter, A.; Makk, P.; Mackowiak, S.; Csonka, S.; Wawrzyniak, M.; Martinek, J. Regular Atomic Narrowing of Ni, Fe, and V Nanowires Resolved by Two-Dimensional Correlation Analysis. *Phys. Rev. Lett.* **2010**, *105*, 266805.
(63) Fock, J.; Sørensen, J. K.; Lörtscher, E.; Vosch, T.; Martin, C. A.; Riel, H.; Kilså, K.; Bjørnholm, T.; van der Zant, H. A Statistical Approach to Inelastic Electron Tunneling Spectroscopy on Fullerene-Terminated Molecules. *Phys. Chem. Chem. Phys.* **2011**, *13*, 14325−14332.
(64) Reuter, M. G.; Hersam, M. C.; Seideman, T.; Ratner, M. A. Signatures of Cooperative Effects and Transport Mechanisms in Conductance Histograms. *Nano Lett.* **2012**, *12*, 2243−2248.
(65) Williams, P. D.; Reuter, M. G. Level Alignments and Coupling Strengths in Conductance Histograms: The Information Content of a Single Channel Peak. *J. Phys. Chem. C* **2013**, *117*, 5937−5942.
(66) Hamill, J. M.; Wang, K.; Xu, B. Force and Conductance Molecular Break Junctions with Time Series Crosscorrelation. *Nanoscale* **2014**, *6*, 5657−5661.
(67) Bâldea, I. Interpretation of Stochastic Events in Single-Molecule Measurements of Conductance and Transition Voltage Spectroscopy. *J. Am. Chem. Soc.* **2012**, *134*, 7958−7962.
(68) Hines, T.; Díez-Pérez, I.; Hihath, J.; Liu, H.; Wang, Z.-S.; Zhao, J.; Zhou, G.; Müllen, K.; Tao, N. Transition from Tunneling to Hopping in Single Molecular Junctions by Measuring Length and Temperature Dependence. *J. Am. Chem. Soc.* **2010**, *132*, 11658−11664.
(69) Nakashima, S.; Takahashi, Y.; Kiguchi, M. Effect of the Environment on the Electrical Conductance of the Single Benzene-1,4-Diamine Molecule Junction. *Beilstein J. Nanotechnol.* **2011**, *2*, 755−759.
(70) Büttiker, M.; Imry, Y.; Landauer, R.; Pinhas, S. Generalized Many-Channel Conductance Formula with Application to Small Rings. *Phys. Rev. B* **1985**, *31*, 6207−6215.
(71) Economou, E. N. *Green's Functions in Quantum Physics*, 3rd ed.;Springer-Verlag: Heidelberg, Germany, 2006.
(72) Ghahramani, S. *Fundamentals of Probability*, 2nd ed.; Prentice-Hall: Upper Saddle River, NJ, 2000.
(73) MolStat. https://bitbucket.org/mgreuter/molstat (accessed February 1, 2015).
(74) Caprio, M. A. LevelScheme: A Level Scheme Drawing and Scientific Figure Preparation System for Mathematica. *Comput. Phys. Commun.* **2005**, *171*, 107−118.

DOI: 10.1021/jp5093515
J. Phys. Chem. C XXXX, XXX, XXX−XXX